Available online at www.sciencedirect.com

ScienceDirect

Procedia Engineering 00 (2016) 000–000

Procedia Engineering

www.elsevier.com/locate/procedia

1st International Conference on the Material Point Method, MPM 2017

Preliminary results of instrumented laboratory flow slides

Richard R. de Jager[a,b,*], Arash Maghsoudloo[a], Amin Askarinejad[a], Frans Molenkamp[a]

[a]*Delft Univerity of Technology, Stevinweg 1, 2628 CN, Delft, the Netherlands*
[b]*Royal Boskalis Westminster, Rosmolenweg 20, 3356 LK, Papendrecht, the Netherlands*

Abstract

The liquefaction tank is an experimental facility developed to conduct physical scale model tests of liquefaction flow slides. We developed the liquefaction tank to evaluate the performance of advanced numerical models for submerged slopes composed of sand. For the long-term, the research with the liquefaction tank aims at composing a database with high-quality experimental results of liquefaction flow slides, in which properties related to the soil, degree of saturation, geometry, triggering and mitigating measures will be varied. This paper addresses the first results obtained with the liquefaction tank. We used a fluidization system to create a uniform, loosely packed sand bed. The liquefaction tank was subsequently tilted uniformly, while measuring the pore pressures at the base of the sand bed. Furthermore, the stability of the slope was monitored using a camera system pointed at the transparent side of the tank. We conducted around 30 tilting tests on a level sand bed while varying consolidation time, density and tilting rate. We were able to reproduce liquefaction flow slides below a particular threshold density. The moment of failure was noted by an instant, uniform liquefaction of the sand bed, preceded by an abrupt increase of excess pore pressures. The results in terms of failure angle and measured pore pressures were consistent and reproducible. The measured failure angle was much lower than anticipated from results of element tests (e.g. triaxial tests) in literature. Future research aims at relating the results to the response during undrained triaxial tests and the effect of mitigating measures.

Peer-review under responsibility of the organizing committee of the 1 st International Conference on the Material Point Method.

Keywords: liquefaction; flow slide; scale model test.

* Corresponding author. Tel.:+31 786969448.
E-mail address: Richard.de.jager@boskalis.com

Peer-review under responsibility of the organizing committee of the 1 st International Conference on the Material Point Method.

1. Introduction

Liquefaction flow slide [1,13] is the main geohazard for subaqueous slopes composed of loose sand. During a liquefaction flow slide the sand instantly transforms from a solid-like to a liquid-like behaving material. The large reduction in shear strength produces a mechanism that may be initiated by a minor trigger, develops rapidly and displaces large volumes of sand over vast distances. It is no surprise that some of the most destructive failures in the history of geotechnics were liquefaction flow failures. For an overview of case histories one is referred to [1].

The currently available methods for assessing liquefaction flow slides [2-5] are unsatisfactory for the complex problems that arise in engineering practice. We attribute this shortcoming to a few factors: the variable state of the subsoil and the lack of means to determine its *in-situ* properties, the coupled and highly non-linear response of the soil during flow liquefaction and the lack of detailed information from case histories. The common methods tend to simplify and decouple the assessment, while relying on a limited, empirical basis. Considering the aforementioned factors, these methods have a narrow range of application with uncertain results outside this range.

As an alternative, more advanced methods, for instance based on the Finite Element Method or related methods, can be employed to assess liquefaction flow slides. These methods are potentially capable of capturing the soil response in detail from the moment a flow slide is triggered to the moment of re-sedimentation at a gentle slope. However, more advanced methods also require a firm basis to verify and validate the results. To this end, the liquefaction tank was developed. The liquefaction tank is a large-scale experimental equipment that facilitates model tests of flow slides. On the long term, the development of the liquefaction tank aims at compiling an open source, high-quality experimental database that can be used by researchers to test the performance of numerical models.

This paper will present the first, preliminary results obtained with the liquefaction tank. The test series were conducted to demonstrate that the liquefaction tank is capable of producing consistent and reproducible data of liquefaction flow slides. The paper will first introduce the set-up by addressing the basis of design, the structure of the tank, the fluidization system, triggering mechanisms and instrumentation. Then, we will discuss the preliminary test results, including details of the testing program and the typical measured response of the soil. The paper will discuss these results in the final section and will draw the future perspectives on the experimental data collection by means of the liquefaction tank.

2. The liquefaction tank

2.1. Basis of design

Physical model tests leave the option of conducting tests in a *1g*-set up or a centrifuge model. We preferred the former for a number of reasons. The preparation of a very loosely packed, uniform sand bed in the centrifuge test is complicated by limited options for preparation techniques, vibrations during spinning up and non-uniformities at higher g –levels [6]. The required scaling of the hydraulic conductivity of the saturated soil using a pore fluid with an increased viscosity also affects the free water next to the slope [7-8]. As a consequence, the artificially induced support by the free water will affect the response, particularly at larger deformations. If flow liquefaction is triggered by creep, as observed in element tests, the yet unresolved scaling of creep time complicates flow liquefaction slides in the centrifuge [9]. The same accounts for erosion and sedimentation during the post-liquefaction phase, which lacks experimental validation.

There are only a few, reported cases of physical model tests of liquefaction flow slides in subaqueous slopes [10-12], where we ignore the well-referenced work by Eckersley [13] which concerns unsaturated slopes. Apart from the limited amount of testing, the results lack detailed documentation, control over the preparation of the sand bed and specification of the trigger. Questions have been raised on the reproducibility of the measured response, while particularly the first phase of the liquefaction flow slides was not well-defined. During the development of the liquefaction tank particular attention was paid on the preparation of the sand and the specification of the trigger. In addition, it is recognized that element tests are needed for the interpretation of the measured response and possible extrapolation to field conditions. The main requirements defined during the development of the liquefaction tank are defined as follows:

- The sand bed should be susceptible to flow liquefaction, while noting that the stress levels are expected to be significantly lower than in field conditions. For the sake of reproducibility, the density of the sand bed should be uniform and known.
- The trigger should be sufficiently large to initiate flow liquefaction and should be well-defined at each stage of the mechanism.
- The conditions in the liquefaction tank should be reproducible in element tests, that is, the intergranular fabric after preparation and stress levels should be similar in both cases. The minimum normal stress level that can be established with reasonable accuracy (error less than 5%) in element tests on loose, fully-saturated sand samples is estimated in the range from about 2 to about 11 kPa [20].

2.2. Structure of the tank

The structure (Fig. 1) comprises the base frame, tank frame, glass sheets and components connecting these. The base frame enables the tank frame to be rotated (see section 2.4). Isolators supporting the base frame only allow the passing of externally induced vibrations with frequencies well below the Eigen frequency of the very loose sand layers and slopes in the liquefaction tank. A pair of hinges and jack-up screws connect the base frame to the tank frame. The tank frame consists of a steel frame with steel plates at the ends and glass sheets at the sides. On top of one of the end plates an overflow basin has been welded, which has been connected to a filtering system in the basement. Two pumps recirculate the water through the system during preparation of the sand bed by means of fluidization. The tank frame measures (length x width x height) 5 x 2 x 2 m. We selected the height based on the required stress level (see section 2.1), the length based on a particular distance of the sand to run out freely and the width based on a minimization of lateral boundary effects. The glass sheets at the sides are constructed from hardened glass in one piece, thereby minimizing the friction at the sides. Rubber wrapped around the edges protects the sheets from point loads. However, the rubber also caused problems when sealing the liquefaction tank. The leakage of water caused severe delays during the construction of the tank.

2.3. Fluidization system

In the liquefaction tank, fluidization is used to prepare the sand bed in a loose and uniform state. The fluidization system consists of ten perforated PVC tubes at the bottom, overlain by two granular filter layers and synthetic filter layers separating the different types of granular layers. The fluidization process is controlled by controlling the flow rate of water pumped into the system. The main design requirement of the fluidization system is to provide a uniform pressure at the bottom, which is expected to provide a uniformly packed sand bed. However, the flux of water from the fluidization system into the tank will result in a gradient in terms of pressure along the fluidization system. We selected the properties of the fluidization system based on a numerical analysis [14]. The actual pressure gradient was later verified during a series of fluidization tests and considered satisfactory.

The sand bed in the liquefaction tank can be further prepared by dredging a slope. However, this paper addresses tests that were conducted on a level bed, so no further attention will be paid to the dredging machine.

2.4. Triggers

The interpretation of case histories of liquefaction flow slides is hampered by a lack of information on the triggers. Liquefaction flow slides are often only noted after occurrence, which is attributed to the fact that liquefaction is triggered under water and out of sight, and often occurs unexpectedly. The aforementioned, reported physical model tests seem to be directed at the process following initiation rather than the triggering itself. In order to define the properties of the load during triggering unambiguously, it should either be imposed to the whole mass or monitored in detail. The liquefaction tank was designed to test several types of triggers. In this paper we will concentrate on triggering by rotating the whole tank frame using the jack-up screws. These are connected by a cross beam to ensure the tank is lifted equally at both lateral sides. The engine controlling the jack-up screws can impose

different tilting schemes, including sudden halting. During the preliminary test series the rotation rate of the tank was held constant.

2.5. Instrumentation

Fig. 1 provides an overview of the instrumentation in the liquefaction tank, numbered according to type. The following sensors are installed [15]:

- Three fluid pressure sensors at the bottom (1);
- Two fluid pressure sensors at each of the two end platens (2,3);
- Two compensated total load sensors (4);
- A differential pressure sensor (5), flow meter and fluid pressure sensor (not depicted) in the fluidization system;
- An accelerometer and temperature sensor at the frame (6,7);
- Six measurement tapes at each side of the tank (not depicted).

Sensors measuring fluid pressure and accelerations in the sand bed have been developed, but were not used during the test series discussed in this paper. Here, we will mainly consider the measurements obtained from the sensors in the bottom (1).

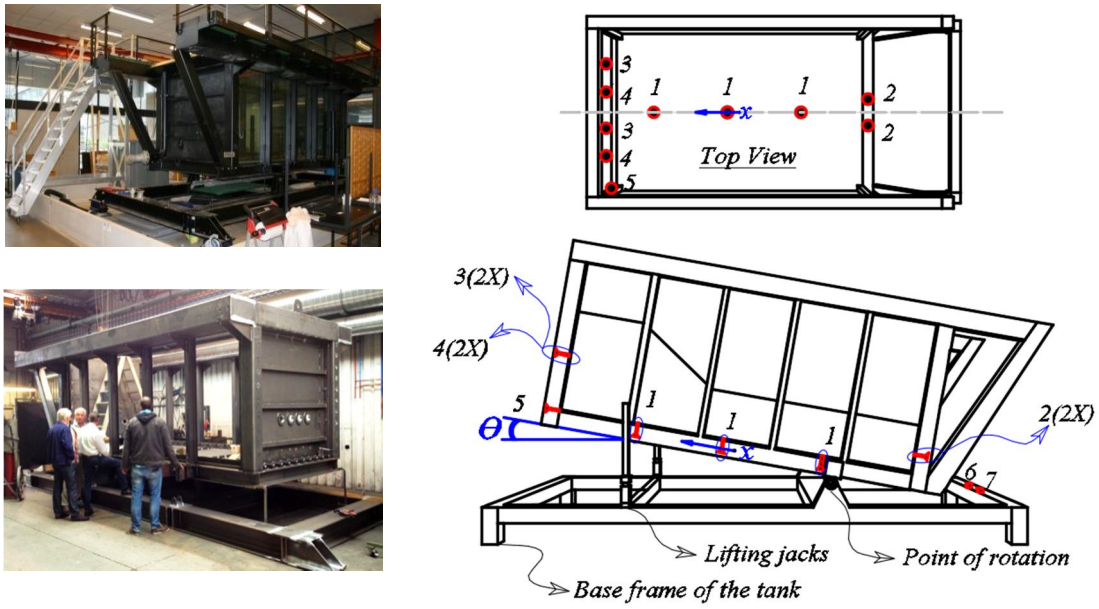

Fig. 1. (a) The liquefaction tank (b) Overview of instrumentation in the liquefaction tank.

3. Preliminary test results

3.1. General

For the first test series the liquefaction tank was filled with approximately 7.5t of sand resulting in an overall bed height of approximately 0.5m. The sand used for the tests concerns a subrounded, uniform fine sand with a D_{50} of 125µm and coefficient of uniformity D_{60}/D_{10}=1.35. Before starting the testing the sand bed was extensively flushed using the fluidization system and overflow to remove any fines. This process was monitored by retaining and storing

the soil that was removed. By weighing the mass of the dry soil before it was moved into the tank and the mass of the soil that was removed during flushing, we were able to back calculate the sand left in the tank [16]. The internal measures of the tank then define the volume of the sand bed and, thereby, the density of the sand. We carried out an error analysis on both the measured soil mass and the volume of the sand bed to determine the accuracy of the resulting density. The established error varies with the height of the sand bed. Generally, the error in terms of dry density is within 1%, which is considered acceptable. During testing, the height of the sand bed was monitored using the measurement tapes to determine the density, which is an average measure of the whole sand bed.

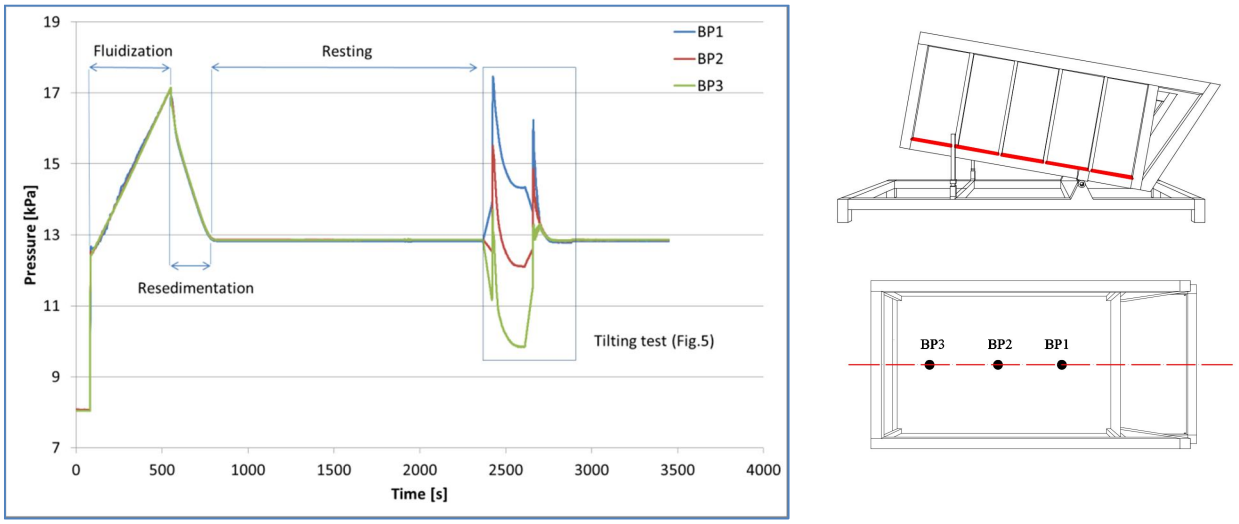

Fig. 2. Fluid pressure response measured at the bottom of the liquefaction tank during fluidization and tilting.

The test series comprised 30 tests in total. All tests started with a fully submerged sand bed that was fluidized during the first stage. By varying the flow rate and duration of fluidization different densities could be established, albeit within a limited (loose) range. In some cases, short periods (5s) of fluidization hereafter established higher densities. The range of established porosities obtained in this way was n=0.443-0.482. The reported results in this paper are from test TT17, which was conducted at a porosity of n=0.481, to illustrate the response of the sand bed. Fig. 2 shows the pressure response at the bottom for the whole test duration.

It is noted that the water level before and after fluidization was well below the overflow, as the capacity of the overflow would have been insufficient to cope with the discharge during the applied rate of rotation of the tank. After resedimentation of the loose sand started the pore pressures dissipated within a few minutes, after which the sand bed was left to rest for at least 20 min. We also varied the time in between fluidization and tilting of the tank to investigate possible time effects (“ageing”), but these will not be addressed in this paper. Next, the tank was tilted at a constant rate of rotation of 0.11°/s to a final tilting angle of 10° with the horizontal. In this paper we will discuss the measured pore fluid pressures at the bottom of the tank. The pore pressures in Fig. 2 instantly increase as the fluidization system is turned on, which indicates that a state of fluidization (zero effective stress) is instantly reached. The subsequent, gradual rise in pressures is attributed to the rise in water level during fluidization. After a period of consolidation and waiting (resting phase in Fig. 2) the tank is tilted. The pore pressures first gradually change, but suddenly increase as flow liquefaction is triggered. After a peak, consolidation of the soil reduces the pore pressures. The tank is held in position for a short while, after which it is tilted reversely to its original, horizontal position. During this stage, the soil again shows an increase in excess pore pressures. The excess pore pressures during tilting will be considered in more detail in section 3.3.

3.2. Observed response

Fig. 3 shows the typical observed response at four successive moments in time. A test conducted after the test series discussed here has been depicted, but the observed response is essentially the same for all tests in which the sand bed liquefied. The first frame shows the initial sand bed before tilting started, the second frame depicts the still stable sand bed during tilting. Then, instability of the sand bed is first noted at the lower side of the liquefaction tank, where the sand bed levels, followed by a wave propagating to the upper side of the tank. Finally, the whole sand bed is levelled (fourth frame) indicating that the soil has a negligible liquefied strength. The depicted process in post-instability frames 2 to 4 takes around 10s.

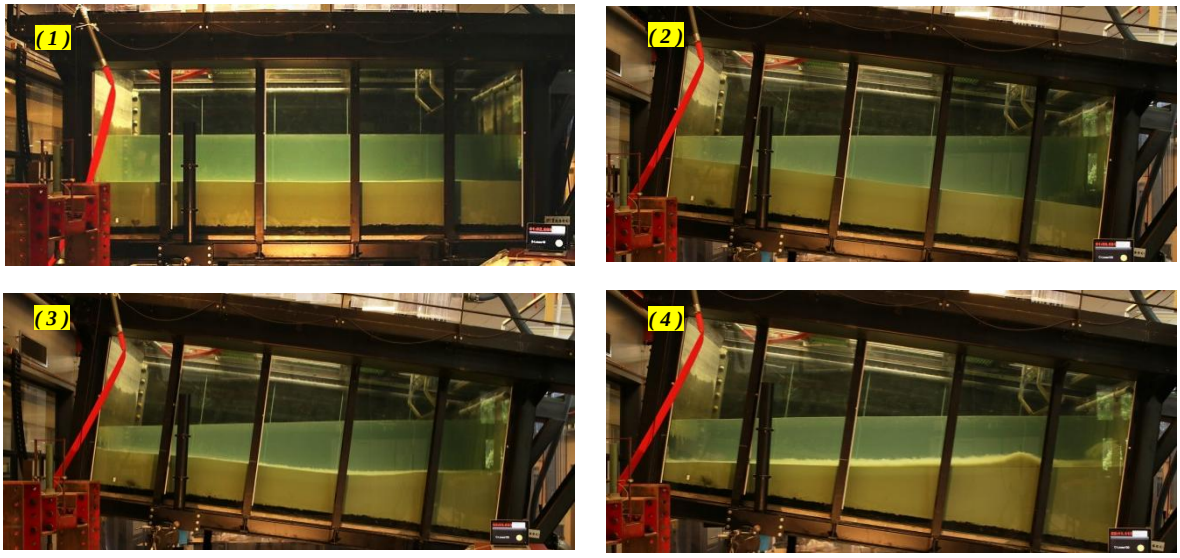

Fig. 3. Four subsequent characteristic frames of submerged very loose sand bed during tilting of liquefaction tank.

It is hard to define the exact moment of instability from observing the sand bed. As an alternative, we consider the excess pore water pressures as measured at the bottom of the tank in the next section.

3.3. Excess pore pressure response

The excess pore water pressure p_{exc_k} (k=1,2,3) for each of the three measured pore pressures p_k in the bottom of the liquefaction tank by means of sensors BP1, BP2 and BP3 (see Fig. 2) during monotonically increasing tilting of the liquefaction tank over angle θ are calculated by

$$p_{exc\_k} = p_k - p_{h\_k} = p_k - \left(p_{0\_k} \cos\theta - x_k \gamma_w \sin\theta \right) \tag{1}$$

in which p_{h_k} is the calculated instantaneous pore water pressure at the location of the sensor if the instantaneous pore water pressure distribution would remain hydrostatic, p_{0_k} is the measured initial pore water pressure of the sensor before the start of tilting (θ=0), when the pore water pressure distribution is still hydrostatic, γ_w is the volumetric weight of the (pore) water and x_k indicates the location of the sensor along the bottom of the liquefaction tank with respect to the centre of this bottom and with positive direction as illustrated in Fig. 1.

Fig. 4 depicts the result, where the tilting profile of the tank has been plotted on the secondary vertical axis. The tilting increases the excess pore pressure slightly by 0.1kPa or less. Then, at a tilting angle of approximately 6.3° the excess pore pressures instantly and simultaneously rise marking the start of instability. The movement of the sand bed starts affecting the pressure readings just after peak. Furthermore, the failure has an effect on the water level as well, as can be observed from the wave patterns in the pressure response. The tilting of the tank back to its original position also yields an instant increase of pore pressures, albeit to a lesser extent than the first peak. The same accounts for the visually observed bed response, which shows some small, occasional instabilities instead of a uniform instability of the bulk mass.

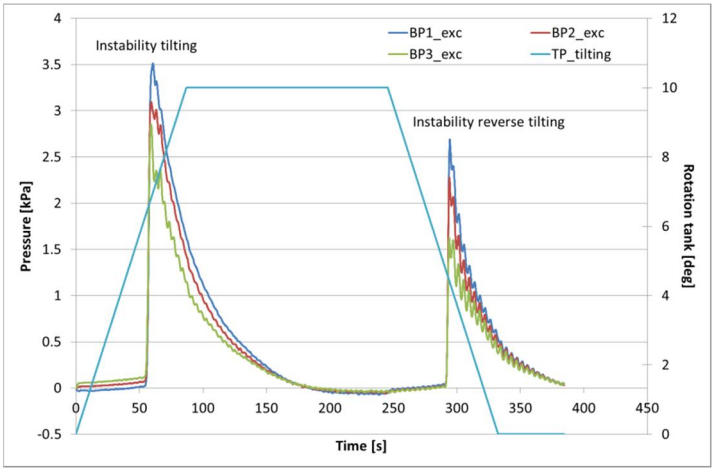

Fig. 4. Excess pore pressures and rotation of tank during tilting test.

4. Discussion of the results

The test results shown in Fig. 2 and Fig. 4 demonstrate that the liquefaction tank is capable of reproducing liquefaction flow slides. The excess pore pressure readings seem to provide a proper indication for the start of failure, as the readings are affected by the movement of the sand bed just after the peak. The abrupt increase in pore pressure coincides for the three sensors, which makes it impossible to determine where flow liquefaction is initiated. To this end, measurement should be taken in the sand bed and at a high frequency. The failures were triggered under essentially drained conditions. The rate of rotation is sufficiently low to allow drainage as can be seen by the negligible excess pore pressures during the first stage of rotation. We measured the accelerations of the base frame during one of the tests to verify whether vibrations induced during tilting could have initiated liquefaction. The accelerations were negligible and vibrations are excluded as a possible initiation for liquefaction.

Moreover, the other tests demonstrate that the results are reproducible; the rotation angle at which the excess pore pressures abruptly increase has been shown to be practically identical for the same densities. This rotation angle, which is denoted by the “failure angle”, increases linearly with increasing density. For the full range of densities that was tested, excess pore pressures were measured. The magnitude of excess pore pressures decreased linearly with increasing density. However, below a porosity of n=0.465 failure of the sand bed was no longer observed. Apparently, the generation of excess pore pressures alone is not a proper indicator for flow failures.

Flow failures were initiated at a failure angle between 5.9° and 7.1°, corresponding to a slope of 1v:8h to 1v:10h. These values are much lower than deducted from element tests. For instance, the instability line [18], which is a measure for the start of instability during an undrained triaxial test, is usually measured at a mobilized friction angle around 15° [3]. Failures at gentle, subaqueous slopes have been observed in practice, but are often attributed to complex mechanisms such as void ratio redistribution. We believe that the measured response in the liquefaction tank is simply the result of the soil behavior itself. Considering the small excess pore pressures before failure and the absence of a clear, external trigger, creep seems to be a probable trigger for the tests in the liquefaction tank.

5. Future perspectives

Future investigations are required to gain better understanding of the mechanism underlying the static liquefaction phenomena and develop reliable analytical and numerical models. To this end, the research team will focus on next level of experimental plans. In the next step, a suction based dredging system will be utilized in the liquefaction tank to create and test slopes. In addition, forming a slope in the liquefaction tank will enable us to investigate the post-failure large displacements. The outcome of displacement monitoring will be a rich database for evaluation of Material Point Method based models. Additional floating acceleration and pore pressure sensors will be installed in the soil body to characterize the displacement behavior and pore pressure generation at the onset of static liquefaction. Innovative element tests are planned to be performed for soil advanced characterization and determination of the parameters for advanced numerical models dealing with liquefaction. In future research, to provide additional evidence for instability different tilting rates and stress states will also be investigated in the liquefaction tank.

Acknowledgements

This research was supported by the Dutch Technology Foundation STW, which is part of the Netherlands Organization of Scientific Research (NWO) and which is partly funded by the Ministry of Economic Affairs, Agriculture and Innovation. We are also grateful for the support by the Royal Boskalis Westminster N.V. for this research and for the support by Rijkswaterstaat [17], enabling the continuation of this research in order to address research questions related to the design of mitigation measures for the prevention of the occurrence of liquefaction in existing hydraulic engineering structures.

References

[1] M. Jefferies and K. Been, Soil liquefaction: a critical state approach, first ed., Taylor & Francis, New York, 2006.
[2] I. Idriss and R. Boulanger, Soil liquefaction during earthquakes, Earthquake engineering research institute, 2008.
[3] J. Chu, S. Leroueil, and W. Leong, Unstable behaviour of sand and its implication for slope instability, Can. Geot. J. 40 (2003), 873-885.
[4] S. Olson and T. Stark, Yield strength ratio and liquefaction analysis of slopes and embankments, J. Geot. Geoenv. Eng. 129 (2003), 727-737.
[5] S. J. Poulos, G. Castro, and J.W. France, Liquefaction evaluation procedure, J. Geot. Eng. 111 (1985), 772-792.
[6] S.-S. Park and P. Byrne, Stress densification and its evaluation, Can. Geot. J. 41 (2004), 181-186.
[7] A. Askarinejad, A. Beck, and S.M. Springman, Scaling law of static liquefaction mechanism in geo-centrifuge and hydro-mechanical characterisation of an unsaturated silty sand having a viscous pore fluid. Can. Geot. J. 52 (2015), 1-13, doi:10.1139/cgj-2014-0237.
[8] A. Askarinejad, J. Laue, A. Zweidler, M. Iten, E. Bleiker, H. Buschor, and S.M. Springman, Physical modelling of rainfall induced landslides under controlled climatic conditions. In Eurofuge Delft, Netherlands, Doi:10.4233/uuid:8105d54f-89af-49b9-9eb1-99e8f5729527.
[9] J. Garnier, G. Gaudini, S. Springman, P. Culligan, D. Goodings, D. Konig, B. Kutter, R. Phillips, M. Randolph, and L. Thoreli, Catalogue of scaling laws and similitude questions in geotechnical centrifuge modelling, Int. J. Phys. Mod. Geot. 3 (2007), 1-23.
[10] M. De Groot, J. Lindenberg, D.Mastbergen, and G. van den Ham, Large scale sand liquefaction flow slide tests revisited, in Eurofuge, Delft, the Netherlands, 2012, 1–22.
[11] F. Molenkamp and R. van Os, Liquefaction test in the Brutus Tank, Tech. Rep. COSE-690504/2, Delft Geotechnics, Delft, 1987.
[12] A. Bezuijen and D. Mastbergen, On the construction of sand fill dams—part 2: Soil mechanical aspects, in: P. Kolkman, J. Lindenberg, and K. Pilarczyk (eds.), International Symposium on Modelling of Soil-Water-Structures Interactions, Balkema, Rotterdam, 1988), pp. 363–371.
[13] D. Eckersley, Instrumented laboratory flowslides, Géotechnique 40 (1990), 489-502.
[14] R. de Jager and F.Molenkamp, Fluidization system for liquefaction tank, in Eurofuge, Delft, the Netherlands, 2012, Doi: 10.4233/uuid:47ce6506-b678-46ee-be42-414cc1a00d69.
[15] R. van den Oever, J. Graafland, R. de Jager and F. Molenkamp, Instrumentation and control of experiments in liquefaction tank , Int. rep., Delft Univ. of Tech., 24-01-2013.
[16] F. Molenkamp and R. de Jager, Determination of global sand density in liquefaction tank, Int. rep., Delft Univ. of Tech., 2-8-2015.
[17] A. Maghsoudloo, A. Askarinejad, M. Hicks, Role of scour protection on prevention of static liquefaction induced flow slides, Int. rep., Delft Univ. of Tech., 26-6-2016.
[18] P. Lade, Static instability and liquefaction of loose fine sandy slopes, J. Geot. Eng. 118 (1992), 51-71.
[19] T. Kokusho, Current state of research on flow failure considering void redistribution in liquefied deposits, Soil Dyn. Earthq. Eng. 23 (2003), 585-603.
[20] R. de Jager, F. Molenkamp, Characteristics of sensors and control of triaxial equipment for saturated sand samples prepared by fluidization, Int. rep., Delft Univ. of Tech., 11-3-2015.